PROCEEDINGS OF SPIE

SPIEDigitalLibrary.org/conference-proceedings-of-spie

Absorption sensing enhancement in a microresonator coupled to a non-adiabatic tapered fiber

A. T. Rosenberger

A. T. Rosenberger, "Absorption sensing enhancement in a microresonator coupled to a non-adiabatic tapered fiber," Proc. SPIE 10548, Steep Dispersion Engineering and Opto-Atomic Precision Metrology XI, 105480G (22 February 2018); doi: 10.1117/12.2299193

SPIE.

Event: SPIE OPTO, 2018, San Francisco, California, United States

Absorption sensing enhancement in a microresonator coupled to a non-adiabatic tapered fiber

A. T. Rosenberger*
Department of Physics, Oklahoma State University, Stillwater, OK, USA 74078-3072

ABSTRACT

Whispering-gallery microresonators are well suited for use as sensors. For example, fluid analytes can be sensed through their effect on the refractive index or by their optical absorption. The former results in a frequency shift of a whispering-gallery mode (WGM); the latter changes the WGM's intensity profile, and can be even more sensitive than the former. WGMs are typically excited by coupling of light from a tapered fiber. It has recently been demonstrated that using a non-adiabatic tapered fiber can produce a Fano resonance whose asymmetric shape can enhance the sensitivity of refractive-index sensing. The non-adiabatic taper allows the incoming light to be distributed between two fiber modes that interfere when exciting a single WGM, thereby producing the asymmetric resonance. However, just as absorption sensing can be more sensitive than index sensing, its enhancement by using a non-adiabatic taper can be greater as well. This enhancement is demonstrated theoretically here, and experiments for confirmation are underway.

Keywords: microresonator, whispering-gallery modes, chemical sensing, non-adiabatic tapered fibers

1. INTRODUCTION

Tapering of an optical fiber to a diameter of a few microns or less makes the evanescent component of the light that it carries available for use in sensing or in coupling to whispering-gallery microresonators. In the taper transition, the core-cladding guidance of the untapered fiber evolves to the cladding-air guidance of the waist region, where the evanescent field makes the effective refractive indices (or propagation constants) of the thinned fiber modes sensitive to the refractive index of the ambient. If the taper transition is adiabatic, the single mode of the untapered fiber evolves to a single mode of the tapered fiber (waist). However, if the taper transition is not adiabatic, and the angle of the taper transition is large enough, multiple modes of the tapered fiber can be excited. These different modes will have different spatial profiles, with different evanescent fractions, different effective indices, and different propagation constants.[1-4] The resultant beating of different tapered-fiber modes as they propagate along the waist can enhance the sensitivity to the ambient refractive index and enable sensing of index changes resulting from various effects.[5-8]

When a non-adiabatic tapered fiber (or multimode waveguide) is used for coupling to a microresonator,[9-14] the throughput spectral profile of a resonator mode is no longer a symmetric Lorentzian dip, but depends on the relative amplitude and phase of the fiber modes as they couple into a single resonator mode. In particular, if there are two fiber modes and they are neither in phase nor out of phase, the throughput profile can have the shape of a Fano resonance. This scheme is a simpler way to achieve the Fano resonance than through coupled resonator modes.[15-17] The advantage of the Fano resonance is that it can provide a very steep variation of throughput with frequency, and thus an enhanced response to changes in ambient index.[12-16]

We have previously shown that absorption sensing with (adiabatic) fiber-coupled whispering-gallery microresonators can have even better sensitivity than refractive index sensing, while being less susceptible to perturbations arising from intensity or frequency drifts.[18-20] In this paper, the enhancement of absorption sensing that can be provided by non-adiabatic tapered-fiber coupling is demonstrated theoretically. An analytical and numerical model has been developed that assumes an asymmetric tapered fiber consisting of a non-adiabatic downtaper so that two tapered-fiber modes can interact with a single whispering-gallery mode (WGM) of the resonator, along with an adiabatic uptaper to ensure that only the fundamental tapered-fiber mode couples to the untapered-fiber mode for throughput. This model shows that the resulting enhancement can be even greater for absorption sensing than for index sensing.

*atr@okstate.edu; phone 1 405 744-6742; fax 1 405 744-6811; physics.okstate.edu/rosenber/index.html

Steep Dispersion Engineering and Opto-Atomic Precision Metrology XI, edited by
Selim M. Shahriar, Jacob Scheuer, Proc. of SPIE Vol. 10548, 105480G · © 2018
SPIE · CCC code: 0277-786X/18/$18 · doi: 10.1117/12.2299193

2. MODEL AND BASIC RESULTS

The tapered-fiber-coupled microresonator is taken to be analogous to a ring cavity with one partially-transmitting mirror. The mirror transmission gives the coupling from the taper mode to a WGM and back again. The throughput is analogous to the signal reflected from the cavity. The two taper modes are modeled as two orthogonal (spatially; they are assumed to have the same polarization) modes incident on the cavity, having the same frequency but different propagation constants and thus a variable relative phase. As sketched in Fig. 1, light from the single-mode untapered fiber couples into the two waist modes in the non-adiabatic downtaper; these have amplitudes E_{i1} and $E_{i2}e^{i\beta}$ at the point where they couple into the microresonator. The input/output coupling (transmission) coefficients for the two modes are it_1 and it_2. It is assumed that there is no intermode coupling in the adiabatic uptaper, after the microresonator, and that only one of the outgoing taper modes E_{r1} and E_{r2} is recaptured by the untapered fiber core as measurable throughput.

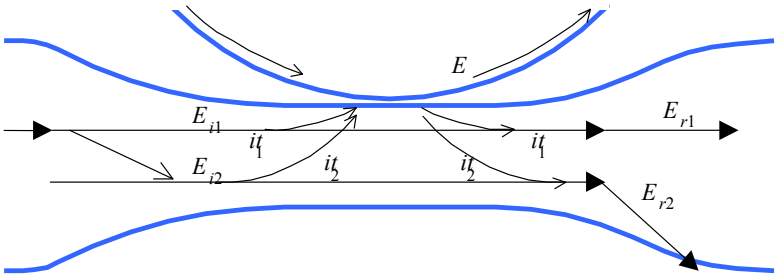

Fig. 1. Multimode coupling. Two tapered-fiber modes couple to a single WGM.

The coupling of incident tapered fiber modes into the WGM is coherent, that is, the amplitude coupled into the WGM is the sum of the complex amplitudes of the coupled portions of the two incident modes. The orthogonality of the taper modes, and the condition that energy be conserved when the cavity has no intrinsic loss, lead to certain relations among the reflection and transmission coefficients. If

$$\begin{aligned} t_1^2 &= 1 - r_1^2, \\ t_2^2 &= 1 - r_2^2, \end{aligned} \tag{1}$$

where it_n and r_n are the transmission and (external) reflection coefficients for mode n, energy conservation requires that

$$1 - r^2 = t_1^2 + t_2^2 = T_1 + T_2, \tag{2}$$

where r is the internal reflection coefficient for the cavity mode and T_n is the transmissivity for mode n. The transmissivities are assumed to be small, i.e., $T_n << 1$.

Consider cw incident waves and steady-state response. E_{i1} and $E_{i2}e^{i\beta}$ are the amplitudes of the two incident modes, with their relative phase β depending on the position of the microresonator along the fiber waist. Then the intracavity WGM mode amplitude E, just after the input coupling, is given by

$$E = \frac{it_1 E_{i1} + it_2 E_{i2} e^{i\beta}}{1 - re^{-\alpha L/2} e^{i\delta}}, \tag{3}$$

where L is the cavity round-trip length, αL is the intrinsic round-trip power loss, and $\delta = kL$ is the round-trip phase accumulation modulo 2π, proportional to the detuning of the incident light from the cavity resonance. Since we assume that no intermode coupling occurs in the second transition region (uptaper), and that mode 2 is lost while mode 1 gets captured by the fiber core, the throughput amplitude of mode 1 becomes

$$E_{r1} = r_1 E_{i1} + it_1 E e^{-\alpha L/2} e^{i\delta} = r_1 E_{i1} - \frac{t_1^2 E_{i1} + t_1 t_2 E_{i2} e^{i\beta}}{1 - re^{-\alpha L/2} e^{i\delta}} e^{-\alpha L/2} e^{i\delta}. \tag{4}$$

However, power is what we measure, so we want the square modulus of this. We can evaluate to lowest order in the small quantities $T_n << 1$, $\alpha L << 1$, $\delta << 1$. The last condition applies because δ is an integer multiple of 2π on any cavity resonance, the cavity Q is very high, and we must be relatively near resonance (within several linewidths). Then we find

$$\left|E_{r1}\right|^2 = \left| \frac{\left(\frac{T_1 - T_2 - \alpha L}{2} + i\delta \right) E_{i1} + \sqrt{T_1 T_2}\, E_{i2} e^{i\beta}}{\frac{T_1 + T_2 + \alpha L}{2} - i\delta} \right|^2 . \tag{5}$$

Far away from the cavity resonance, at large detunings δ, note that the limiting value of $\left|E_{r1}\right|^2$ is $\left|E_{i1}\right|^2$. It is therefore convenient to describe the resonance throughput dip (or peak, or feature, in general) in terms of a relative throughput R; note that a peak means that $R(0) > 1$:

$$R(\delta) = \left| \frac{E_{r1}}{E_{i1}} \right|^2 = \left| \frac{T_1 - T_2 - \alpha L + 2\sqrt{T_1 T_2}\, m e^{i\beta} + i2\delta}{T_1 + T_2 + \alpha L - i2\delta} \right|^2 , \tag{6}$$

where

$$m = \frac{E_{i2}}{E_{i1}}. \tag{7}$$

If $m = 0$ and only one mode is incident on the resonator, the throughput $R(\delta)$ shows the usual feature of a Lorentzian dip at $\delta = 0$. When $m > 0$, the shape of the throughput resonance feature will depend on the values of the parameters. In many cases, $\beta = 0$ will produce a symmetric dip and $\beta = \pi$ will show a symmetric peak. In between these limits, the resonance feature will be asymmetric and can be interpreted as a Fano resonance.

We have produced non-adiabatic asymmetric tapered fibers using a fixed flame brush length and simply pulling the two sides through different distances. While this is not ideal, the resulting non-adiabatic downtaper can excite two waist modes, as verified by observing periodicity in the throughput signal as the microresonator is translated along the fiber waist. For purposes of illustration, the two-mode model has been used to fit experimental throughput resonance feature shapes measured using a 400-μm-diameter microsphere at a wavelength of about 1535 nm. Figure 2(a) shows three peaks, and Fig. 2(b) demonstrates a series of asymmetric lineshapes. In the figure caption, $x_n = T_n/\alpha L$.

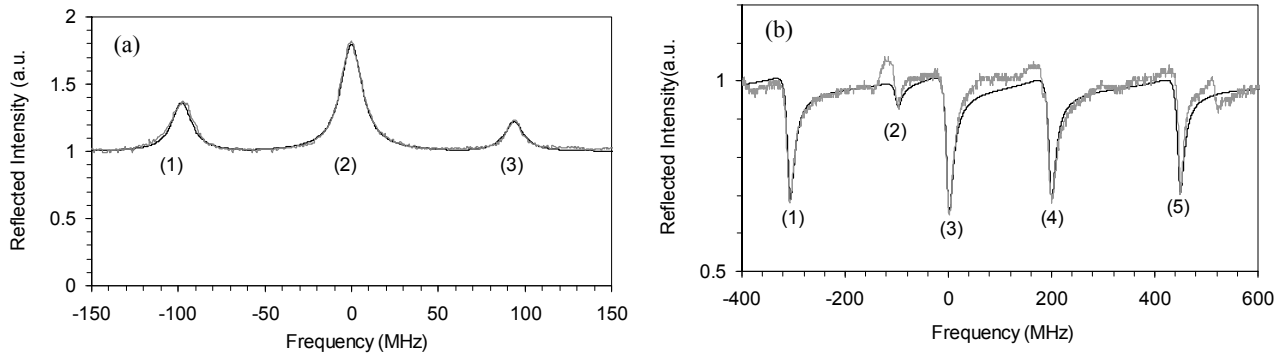

Fig. 2. Experimental results fit by model. (a) Light curve, experimental data. Dark curve, model fit with $m = 4$, $\beta = \pi$, and $\alpha = 0.6$ m^{-1}. The values of x_1 for the (1), (2), and (3) peaks are 0.075, 0.17, and 0.045, respectively. In each case, $x_2 = 0.31\, x_1$. (b) Light curve, experimental data. Dark curve, model fit with $m = 1.4$, $\beta = -0.4\pi$, and $\alpha = 0.70$ m^{-1}. The values of x_1 for the (1), (2), (3), (4), and (5) modes are 0.067, 0.012, 0.075, 0.065, and 0.060, respectively. In each case, $x_2 = 0.31\, x_1$.

For absorption sensing,[18] define the relative throughput dip depth to be $M = 1 - R(0)$, where

$$R(0) = \frac{(T_1 - T_2 - \alpha L)^2 + 4T_1T_2m^2 + 4(T_1 - T_2 - \alpha L)\sqrt{T_1T_2}\,m\cos\beta}{(T_1 + T_2 + \alpha L)^2}. \tag{8}$$

Then suppose that the total loss coefficient becomes $\alpha = \alpha_i + f\alpha_s + f\alpha_a$, where α_i is the resonator's intrinsic loss coefficient, α_a is the absorption coefficient of an analyte in the ambient fluid (gas or liquid), α_s is the absorption coefficient of the ambient solvent (if present), and f is the evanescent fraction of a WGM. Typical values of f are about 10^{-3} in air and 10^{-2} in liquid; these can be larger for internal evanescent fractions in the hollow bottle resonator (HBR).[20]

The measure of absorption sensitivity is the effective absorption path length, given by

$$L_{eff} = \left|\frac{1}{M}\frac{dM}{d\alpha_a}\right| = fL\left|\frac{1}{M}\frac{dM}{d\alpha L}\right| = fL\left|\frac{T_1(T_1 - T_2 - \alpha L) + 2T_1T_2m^2 + (3T_1 - T_2 - \alpha L)\sqrt{T_1T_2}\,m\cos\beta}{(T_1 + T_2 + \alpha L)\left[T_1(T_2 + \alpha L) - T_1T_2m^2 - (T_1 - T_2 - \alpha L)\sqrt{T_1T_2}\,m\cos\beta\right]}\right|. \tag{9}$$

L_{eff} can be as large as f/α in the case of one-mode coupling. With two fiber modes, but $m = 0$, i.e., only the fundamental mode being excited, the maximum effective absorption path length is

$$L_{eff\,\max} = \frac{fL}{T_2 + \alpha L}, \tag{10}$$

so for two fiber modes, when m is greater than zero, the minimum sensitivity enhancement is given by

$$S = \left|\frac{T_2 + \alpha L}{M}\frac{dM}{d\alpha L}\right|. \tag{11}$$

3. MODE PROFILES AND SENSING ENHANCEMENT

In order to compare experimental results to the model described in the previous section, one need only measure the mode linewidth (width of the throughput dip at $\beta = 0$), along with the relative resonant throughput $R(0)$ at $\beta = 0$ and at $\beta = \pi$. From these three measurements, the values of T_1, $T_2 + \alpha L$, and T_2m^2 can be found. These are sufficient for a semiquantitative comparison, as the value of the evanescent fraction can only be estimated to within about a factor of two. The value of f can be calculated for a WGM of known radial order, given the microresonator dimensions, but the radial order of a WGM cannot be determined with certainty. Using an absorbing solvent such as methanol (for the 1500-1650 nm wavelength range) can help to identify the WGM's radial order and/or estimate the value of the evanescent fraction. Note that high sensitivity to α_a is still possible even though $\alpha_a << \alpha_s$; absorption in the solvent just acts as an adjustment to αL.

Two examples of enhancement $S > 1$ are given in Figs. 3 and 4, where R, the ratio of throughput power P_t to mode 1 incident power P_{i1}, is plotted as a function of detuning from the WGM resonance for several values of β. In both examples, the wavelength is taken to be 1500 nm and the loaded Q to be 10^8. In Fig. 3, $T_1/(T_2 + \alpha L) = 1.33$, $m = 1.4$, and $S = 14.1$ for $\beta = 0$. In Fig. 4, $T_1/(T_2 + \alpha L) = 0.273$, $m = 5.8$, and $S = 9.96$ for $\beta = 0$. These enhancements are comparable to that reported for Fano-based index sensitivity.[14] For certain other parameter ranges, absorption sensitivity enhancements as large as 60 have been found; this could increase L_{eff} for gas sensing from about 5 cm to about 3 m.

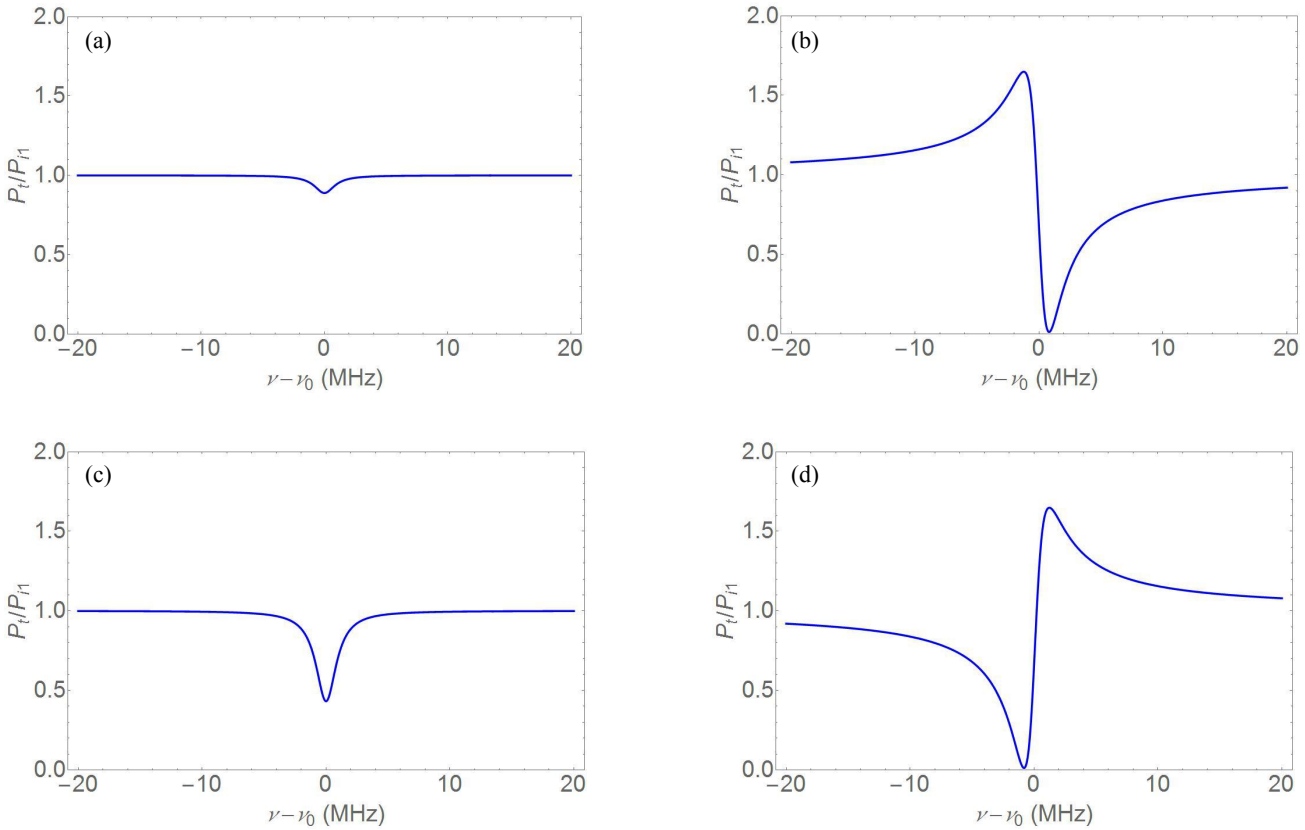

Fig. 3. Mode profiles for different relative phase between the two fiber modes for one case showing absorption sensitivity enhancement. (a) $\beta = 0$. (b) $\beta = 1.5\ \pi$. (c) $\beta = \pi$. (d) $\beta = 0.5\ \pi$. In this case, $T_1/(T_2 + \alpha L) = 1.33$, $m = 1.4$, and $S = 14.1$ for $\beta = 0$.

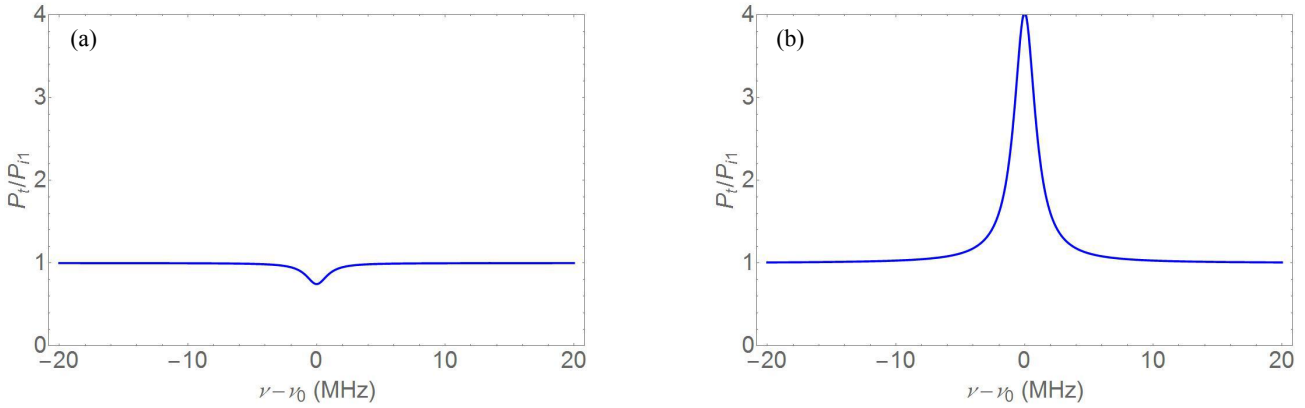

Fig. 4. Mode profiles for different relative phase between the two fiber modes for another case showing absorption sensitivity enhancement. (a) $\beta = 0$. (b) $\beta = \pi$. In this case, $T_1/(T_2 + \alpha L) = 0.273$, $m = 5.8$, and $S = 9.96$ for $\beta = 0$.

4. DISCUSSION

Experiments using non-adiabatic tapered fibers coupled to HBRs are underway to observe the absorption sensing enhancement that has been theoretically demonstrated here. Both liquid and gaseous analytes are being used. One limitation of this method is that large enhancement is often found accompanied by a shallow dip. Using a Fano resonance instead of the throughput dip does not help in absorption sensing. Unfortunately, the large throughput excursion (minimum to maximum) in a Fano resonance such as the $\beta = 0.5\ \pi$ example of Fig. 3(d) seems not to exhibit an enhancement in absorption sensitivity comparable to that of the $\beta = 0$ dip of Fig. 3(a).

REFERENCES

[1] Henry, W. M., and Love, J. D., "Spot size variation in non-adiabatic single mode fibre tapers," IEE Proc. 136, 219-224 (1989).

[2] Love, J. D., Henry, W. M., Stewart, W. J., Black, R. J., Lacroix, S., and Gonthier, F., "Tapered single-mode fibres and devices Part 1: Adiabaticity criteria," IEE Proc.-J: Optoelectron. 138, 343-354 (1991).

[3] Black, R. J., Lacroix, S., Gonthier, F., and Love, J. D., "Tapered single-mode fibres and devices Part 2: Experimental and theoretical quantification," IEE Proc.-J: Optoelectron. 138, 355-364 (1991).

[4] Birks, T. A., and Li, Y. W., "The Shape of Fiber Tapers," J. Lightwave Technol. 10, 432-438 (1992).

[5] Zibaii, M. I., Latifi, H., Karami, M., Gholami, M., Hosseini, S. M., and Ghezelayagh, M. H., "Non-adiabatic tapered optical fiber sensor for measuring the interaction between α-amino acids in aqueous carbohydrate solution," Meas. Sci. Technol. 21**,** 105801 (2010).

[6] Latifi, H., Zibaii, M. I., Hosseini, S. M., and Jorge, P., "Nonadiabatic Tapered Optical Fiber for Biosensor Applications," Photonic Sensors 2, 340–356 (2012).

[7] Muhammad, M. Z., Jasim, A. A., Ahmad, H., Arof, H., and Harun, S. W., "Non-adiabatic silica microfiber for strain and temperature sensors," Sensors and Actuators A 192, 130-132 (2013).

[8] Luo, L., Pu, S., Tang, J., Zeng, X., and Lahoubi, M., "Reflective all-fiber magnetic field sensor based on microfiber and magnetic fluid," Opt. Express 23, 18133-18142 (2015).

[9] Fan, S., Suh, W., and Joannopoulos, J. D., "Temporal coupled-mode theory for the Fano resonance in optical resonators," J. Opt. Soc. Am. A 20, 569-572 (2003).

[10] Chiba, A., Fujiwara, H., Hotta, J., Takeuchi, S., and Sasaki, K., "Fano resonance in a multimode tapered fiber coupled with a microspherical cavity," Appl. Phys. Lett. 86, 261106 (2005).

[11] Ruege, A. C., and Reano, R. M., "Multimode Waveguides Coupled to Single Mode Ring Resonators," J. Lightwave Technol. 27, 2035-2043 (2009).

[12] Ruege, A. C., and Reano, R. M., "Multimode waveguide-cavity sensor based on fringe visibility detection," Opt. Express 17, 4295-4305 (2009).

[13] Ding, D., de Dood, M. J. A., Bauters, J. F., Heck, M. J. R., Bowers, J. E., and Bouwmeester, D., "Fano resonances in a multimode waveguide coupled to a high-Q silicon nitride ring resonator," Opt. Express 22, 6778-6790 (2014).

[14] Zhang, K., Wang, Y., and Wu, Y.-H., "Enhanced Fano resonance in a non-adiabatic tapered fiber coupled with a microresonator," Opt. Express 42, 2956-2959 (2017).

[15] Yu, Z., and Fan, S., "Extraordinarily high spectral sensitivity in refractive index sensors using multiple optical modes," Opt. Express 19, 10029-10040 (2011).

[16] Chao, C.-Y., and Guo, L. J., "Biochemical sensors based on polymer microrings with sharp asymmetrical resonance," Appl. Phys. Lett. 83, 1527-1529 (2003).

[17] Wang, Y., Zhang, K., Zhou, S., Wu, Y.-H., Chi, M.-B., and Hao, P., "Coupled-mode induced transparency in a bottle whispering-gallery-mode resonator," Opt. Lett. 41, 1825-1828 (2016).

[18] Rosenberger, A. T., "Analysis of whispering-gallery microcavity-enhanced chemical absorption sensors," Opt. Express 15, 12959-12964 (2007).

[19] Farca, G., Shopova, S. I., and Rosenberger, A. T., "Cavity-enhanced laser absorption spectroscopy using microresonator whispering-gallery modes," Opt. Express 15, 17443-17448 (2007).

[20] Stoian, R.-I., Bui, K. V., and Rosenberger, A. T., "Silica hollow bottle resonators for use as whispering gallery mode based chemical sensors," J. Opt. 17, 125011 (2015).